coatings

MDPI

Article

Influence of Silicon-Modified Al Powders (SiO_2@Al) on Anti-oxidation Performance of Al_2O_3-SiO_2 Ceramic Coating for Carbon Steel at High Temperature

Bo Yu [1,2], Guoyan Fu [1,3], Yanbin Cui [1], Xiaomeng Zhang [1], Yubo Tu [1,2], Yingchao Du [1,2], Gaohong Zuo [1,4], Shufeng Ye [1] and Lianqi Wei [1,*]

1 State Key Laboratory of Multiphase Complex System, Institute of Process Engineering, Chinese Academy of Sciences, PO Box 353, Beijing 100190, China; yubo@ipe.ac.cn (B.Y.); gyfu@ipe.ac.cn (G.F.); ybcui@ipe.ac.cn (Y.C.); xmzhang@ipe.ac.cn (X.Z.); ybtu@ipe.ac.cn (Y.T.); ycdu@ipe.ac.cn (Y.D.); yglu@ipe.ac.cn (G.Z.); sfye@ipe.ac.cn (S.Y.)

2 Department of Chemical Engineering, University of Chinese Academy of Sciences, No. 19(A) Yuquan Road, Beijing 100049, China

3 China ENFI Engineering Corporation, No. 12 Fuxing Road, Beijing 100038, China

4 Department of Textile and Material Engineering, Dalian Polytechnic University, No. 1 Light Industry Court, Ganjingzi District, Dalian 116034, China

* Correspondence: lqwei@ipe.ac.cn; Tel.: +86-10-8254-4899

Received: 24 January 2019; Accepted: 26 February 2019; Published: 4 March 2019

Abstract: In this paper, silicon-modified Al powders (SiO_2@Al) were prepared by tetraethyl orthosilicate (TEOS) hydrolysis under alkaline conditions. Using SiO_2@Al as additives, a new Al_2O_3-SiO_2 ceramic coating (ASMA) was formed on carbon steel to prevent carbon steel from oxidization at 1250 °C for 120 min. Compared with the Al_2O_3-SiO_2 ceramic coating without additive (AS), ASMA showed a remarkably better anti-oxidation performance, especially during the temperature-rise period. According to the characterization conducted by TG-DTA, XRD and SEM-EDS, it was found that the metallic Al in ASMA melted at 660 °C and reacted with SiO_2 on its surface, which generated local high temperature and accelerated the sintering of ceramic raw materials. The mullite and hercynite formed in ASMA also played a major role for enhancing the anti-oxidation performance of ceramic coating.

Keywords: ceramic coating; anti-oxidation; SiO_2@Al additive; carbon steel

1. Introduction

Carbon steel always involves a slab reheating and hot rolling process to obtain thin carbon steel. During the reheating process, slabs suffer from serious oxidation over 1250 °C, which results in weight loss of slabs and energy waste [1–3]. Moreover, oxidation could potentially lead to serious problems for the surface quality of carbon steel, such as decarburization and micro-defects [4,5]. Different methods have been taken to protect slabs from oxidization during the reheating process. The most effective countermeasure for the reduction of the oxidation intensity is to isolate slabs from oxidants. Therefore, reheating in reducing atmosphere, such as vacuum or inert gas atmosphere, is once thought to be an ideal solution. However, the rigid operation conditions and expensive equipment limit its industrial application [6–8].

Protective coating, an effective and economical method, is considered as an alternative solution to prevent the slabs from oxidization at high temperature [9,10]. Ceramic coating (MgO, Al_2O_3, SiO_2, CoO, ZnO, ZrO_2 etc.) usually has a high melting point and excellent chemical stability at high

temperature [11,12]. By using ceramic coating, a protective layer can be formed on carbon steel surface at temperatures ranging from 1100 to 1300 °C so that the internal diffusion of oxygen and external diffusion of iron ions are slowed down [11,13–16].

Among the ceramic coatings, Al_2O_3-SiO_2 coating (AS) is widely used due to its high anti-oxidation performance and low cost [17]. Silicates with low melting points are always added into Al_2O_3-SiO_2 coating to accelerate the sintering under low temperature. However, a eutectic crystal of Fe–2FeO·SiO_2 is formed over 1170 °C, which is harmful to the anti-oxidation performance of the protective coating at high temperature [18,19]. In order to accelerate the sintering of Al_2O_3-SiO_2 coating under low temperature and avoid the formation of Fe–2FeO·SiO_2 over 1170 °C, silicates with low melting point should be replaced by other additives [20,21]. Aluminite powder is an alternative additive because it can melt at 660 °C and react with SiO_2 [22]. The exothermic reaction between Al and SiO_2 leads to local high temperature and thus the sintering of ceramic materials is accelerated. Sodium silicate and colloidal silica are widely used as binder agents in ceramic coating preparation. Functional colloidal sol would form under the hydrolysis of sodium silicate or metasilicic acid and be balanced with the free OH^-. If Al powders are directly added into ceramic coating slurry containing alkaline binder such as sodium silicate and colloidal silica, a exothermic reaction ($2Al + 2H_2O + 2OH^- \rightarrow 2AlO_2^- + 3H_2$) will take place and break the balance of hydrolysis within the sodium silicate solution ($SiO_3^{2-} + 2H_2O \rightarrow H_2S_iO_3 + 2OH^-$). It was the consumption of OH^- that would accelerate the hydrolysis and enhance the viscosity of the slurry. Viscous slurry is hard to disperse by spraying due to its poor fluidity. In addition, the hydrogen produced by the reaction is flammable and it is hazardous in the reheating workshop. Therefore, Al powders should be modified to be stable with the coating slurry.

In this paper, silicon-modified Al powders (SiO_2@Al) were prepared by tetraethyl orthosilicate (TEOS) hydrolysis under alkaline conditions. A new Al_2O_3-SiO_2 ceramic coating (ASMA) was prepared with SiO_2@Al as additives to prevent carbon steel from oxidization. The anti-oxidation performance of ASMA was investigated by a heating process from room temperature to 1250 °C with a rate of 10 °C/min and maintained for 120 min at 1250 °C. A protective mechanism of ASMA was also clarified. Some achievements in this paper were not only applied to anti-oxidation of carbon steel at high temperature but also provided new ideas for the design of low-temperature sintering ceramic.

2. Experiment Procedure

2.1. Preparation of Carbon Steel Sample

Carbon steel, J55 (C 0.28 wt %, Si 0.27 wt %, Mn 1.35 wt % and Fe balance), with a specimen size of $55 \times 50 \times 5$ mm^3 was used for high temperature treatment in muffle furnace. A carbon steel specimen ($25 \times 24 \times 5$ mm^3) was cut from cold-rolled plates for continuous thermo-balance investigation. The specimens were cleaned with alcohol in an ultrasonic bath and dried in an oven.

2.2. Preparation of Modified Al Powders (SiO_2@Al)

Al powders with the size of 45 μm, tetraethyl orthosilicate (TEOS), ethanol, ammonia water, and deionized water were used for the preparation of SiO_2@Al. A mixture of 10 g Al powders and 250 mL ethanol was stirred in a beaker at 50 °C for 1 h. The mixture was blended with 15 mL TEOS under agitation, which was diluted with 150 mL alcohol. After that, 20 mL ammonia water diluted with 25 mL deionized water was dropped into the mixture by a peristaltic pump at 2 mL/min as the catalyst for TEOS hydrolysis. Then, the beaker was kept in a water bath at 50 °C for 8 h. The obtained SiO_2@Al was separated from the resulting mixture by vacuum filtration, followed by washing several times with ethanol. Then SiO_2@Al was dried at 60 °C under vacuum.

The synthesis of SiO_2@Al through TEOS hydrolysis under alkaline condition is illustrated in Figure 1. The SEM-EDS results in Figure 2 indicated that Al powders were successfully encapsulated

by SiO_2 and thus SiO_2@Al was obtained. The size of SiO_2 encapsulating on the surface of Al powders was about 100 nm.

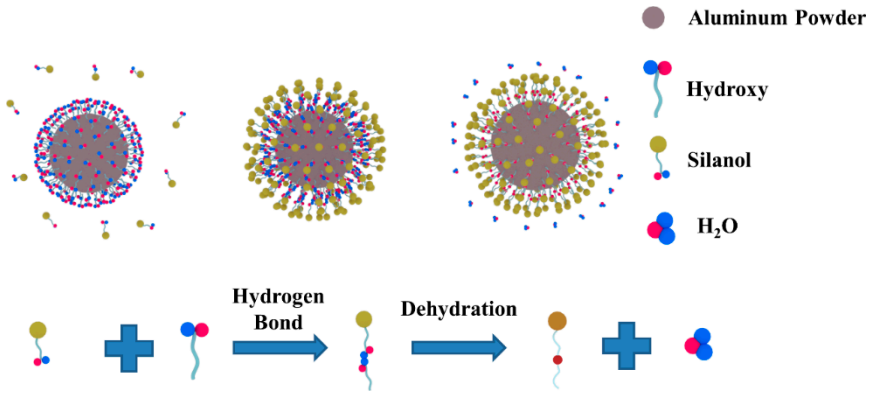

Figure 1. The schematic illustration of SiO_2@Al synthesis.

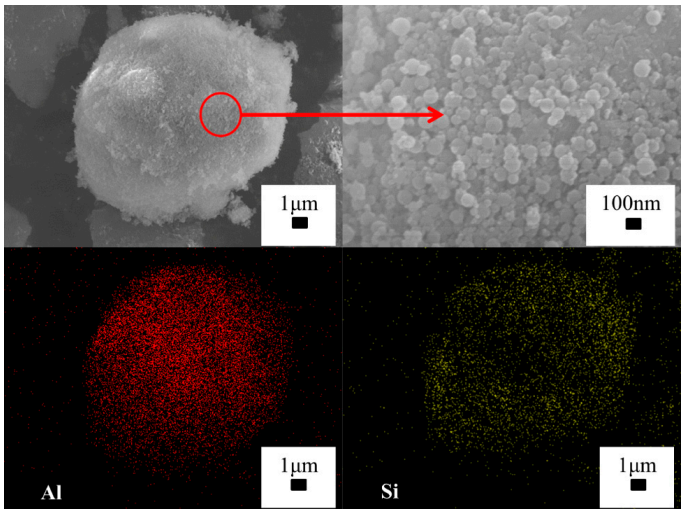

Figure 2. SEM and EDS images of SiO_2@Al.

2.3. Preparation of Coating Slurry

As shown in Table 1, ceramic coating slurry with different amount of SiO_2@Al (0, 5%, 10%, 15%, 20%, 25%) were prepared to determine an appropriate proportion of SiO_2@Al additives. The mixture was ball-milled with water for 4 h until the particle size was <45 μm. The milling ball was ZrO_2 and the diameter of ZrO_2 balls was 6–10 mm. During the ball-milled process, SiO_2@Al stably existed in the slurry without any hydrogen releasing. The prepared slurry was coated on carbon steel by spraying gun, which was connected to an air compressor with pressure of 8 bar. The thickness of the coating was 0.4 mm.

Table 1. The composition of the ceramic coating (wt %).

No.	Al_2O_3	Sodium Silicate Solution (40 wt %)	SiO_2@Al	Surface Active Agent Sodium Polyacrylate	H_2O
1	70.5	23.5	0	4	2
2	66	21	5	4	4
3	62	18.5	10	4	5.5
4	58	16	15	4	7
5	54	13.5	20	4	8.5
6	50	11	25	4	10

2.4. Evaluation of Anti-oxidation Performance

To evaluate the anti-oxidation performance of ceramic coating, the weight changes of heated carbon steel samples were investigated. The carbon steel samples were heated in a muffle furnace from room temperature to different temperatures (1050, 1100, 1150, 1200, and 1250 °C) and maintained for 120 min. The anti-oxidation ability E, which was related to the weight loss of carbon steel oxidation, was calculated by Equations (1) and (2). Two samples were used in each test and the average value of samples was adopted.

$$\text{Steel yield } \alpha = \frac{m_2}{m_1} \times 100\% \quad (1)$$

$$\text{Anti} - \text{oxidation ability } E = \frac{\alpha_{\text{coated}} - \alpha_{\text{bare}}}{1 - \alpha_{\text{bare}}} \times 100\% \quad (2)$$

where, m_1 and m_2 are the weights of samples before and after high temperature treatment without scale. α_{coated} and α_{bare} are the yields of the coated and bare samples after high temperature treatment.

To evaluate the non-isothermal kinetic of carbon steel oxidation, the correlation between oxidation reaction rate and heating temperature was investigated. The samples were heated at a rate of 10 °C/min to certain temperature (1050, 1100, 1150, 1200, and 1250 °C) and maintained for 5 min. The reaction rate (v) was calculated by Equations (3) and (4).

$$\text{Weight loss per unit area } \Delta m = M_2 - M_1 \quad (3)$$

$$\text{Reaction rate } v = \frac{\Delta m}{\Delta t} \quad (4)$$

where, Δm is the weight loss per unit area of the sample during the holding stage at certain temperature. Δt is the time that the samples were maintained at certain temperature.

To evaluate the anti-oxidation ability of ceramic coating at a certain temperature, the isothermal kinetic was also carried out. The isothermal kinetic was conducted by a continuous thermos-balance (RZ, Luoyang Precondar, Luoyang, China) at a heating rate of 10 °C/min to 1250 °C and maintained for 120 min. The weight change of the sample was calculated by Equation (5).

$$\Delta\omega = \omega_i - \omega_0 \quad (5)$$

Here, ω_0 is the weight change per unit area of the sample heated to certain temperature and ω_i is that of the sample heated and maintained at certain temperature.

2.5. Characterization

The morphology of the ceramic coating and carbon steel substrate was characterized by scanning electron microscopy (SEM; JSM-6700F, JEOL, Tokyo, Japan) equipped with an energy dispersive X-ray spectroscopy (EDS, NORAN, Thermo Fisher, Waltham, MA, USA). The phase-transition occurred at different temperature was characterized by X-ray diffraction (XRD; X'Pert Pro, Philips, Amsterdam, The Netherlands) operated from 5° to 90° for 5.25 min. The weight change and thermal change during heating process were detected by TG-DTA (TG-DTA; STA449, Netzsch, Nuremberg, Germany). The TG-DTA test was operated from room temperature to 1250 °C at a heating rate of 10 °C/min. The test was conducted under flowing air.

3. Results and Discussion

3.1. Performance of Coating

The anti-oxidation performances of the coatings with different proportion of SiO_2@Al were investigated by the weight loss during the heating process in muffle furnace. As shown in Figure 3, when temperatures ranged from 1050 to 1150 °C, a higher proportion of SiO_2@Al led to a better

anti-oxidation performance. However, when the proportion exceeded 10%, the enhancement of the anti-oxidation performance was not obvious. When temperatures ranged from 1200 to 1250 °C, the anti-oxidation performance of coating improved with the increasing amount of SiO_2@Al until 10% and reduced with further SiO_2@Al addition, especially at 1250 °C. Therefore, in view of the anti-oxidation performance and the cost, the ceramic coating with 10% of SiO_2@Al was chosen as the appropriate one to conduct the following investigations.

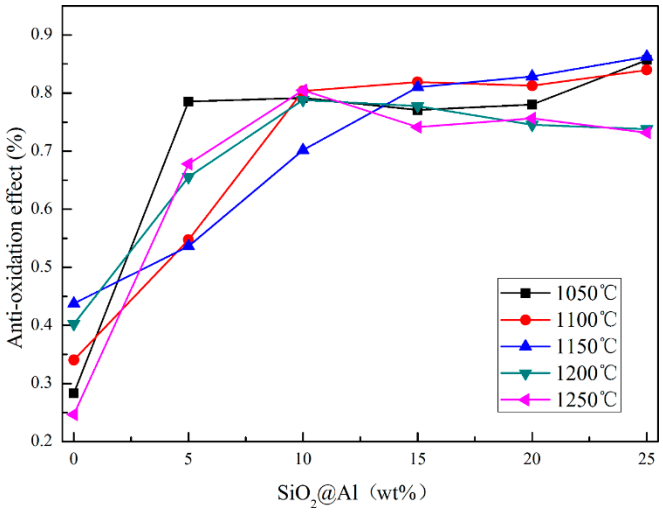

Figure 3. Anti-oxidation performances of the coatings with different proportion of SiO_2@Al.

The non-isothermal kinetic for sample protected by ASMA, sample protected by AS, and bare sample are shown in Figure 4. The apparent activation energy, (E_a), was calculated by the Arrhenius equation. As shown in Equation (6), if the concentration of reactant (B) was constant, the reaction rate (v) would have a positive correlation with the reaction rate constants (k), which is the function of temperature described by Equation (7) (Arrhenius equation).

$$v = B \times \mathrm{k} \tag{6}$$

$$\mathrm{k} = \mathrm{A} \times \mathrm{e}^{(E_a/RT)} \tag{7}$$

The relationship between reaction rate (v) and apparent activation energy (E_a) could be deduced with Equations (6) and (7) by a logarithmic operation. The ultimate equation was described as Equations (8) and (9).

$$\ln \mathrm{k} = -\frac{E_a}{\mathrm{R}T} + \ln \mathrm{A} \tag{8}$$

$$\ln v = -\frac{E_a}{\mathrm{R}T} + \ln \mathrm{A} + \ln \mathrm{B} \tag{9}$$

where, A and B were constant. R was 8.314 $\mathrm{J \cdot mol^{-1} \cdot K^{-1}}$.

Therefore, the dependent variable ($\ln v$) had a linear relationship with the variable ($1/T$). As described in Equations (3) and (4), the reaction rate (v) could be calculated by the weight loss per unit area and the duration time of samples heated to a certain temperature. Based on the kinetic results at different temperatures as shown in Figure 4, a linear relationship was observed between $\ln v$ and $1/T$. The slope of each fitting was equal to ($-E_a/\mathrm{R}$) as described in Equation (8). It was a remarkable fact that the result of the sample protected by AS was not able to be fitted by a single linear equation because there was an inflection point at about 1150 °C. Therefore, the kinetic of the sample protected by AS should be divided into two parts (AS1 and AS2) by 1150 °C.

As shown in Figure 4, the apparent activation energy (E_a) of bare sample was 120.11 kJ/mol, while that of the sample protected by ASMA was 326.50 kJ/mol. The apparent activation energy (E_a)

of the sample protected by AS between 1025 and 1150 °C was 106.14 kJ/mol, which was approximate to the bare sample. The apparent activation energy (E_a) of the sample protected by AS between 1150 and 1250 °C was 224.05 kJ/mol, which was between that of the sample protected by ASMA and the bare sample. Generally, higher apparent activation energy resulted in a better anti-oxidation performance of coating. Therefore, ASMA exhibited an excellent anti-oxidation performance between 1025 and 1250 °C, while AS only worked above 1150 °C. Additionally, the anti-oxidation performance of ASMA was much better than AS due to its larger apparent activation energy (E_a). To further prove the enhancement of anti-oxidation of ASMA, the non-isothermal experiment was conducted by a continuous thermo-balance. As shown in Figure 5, compared with AS, ASMA showed an obviously better anti-oxidation performance during the temperature-rise period.

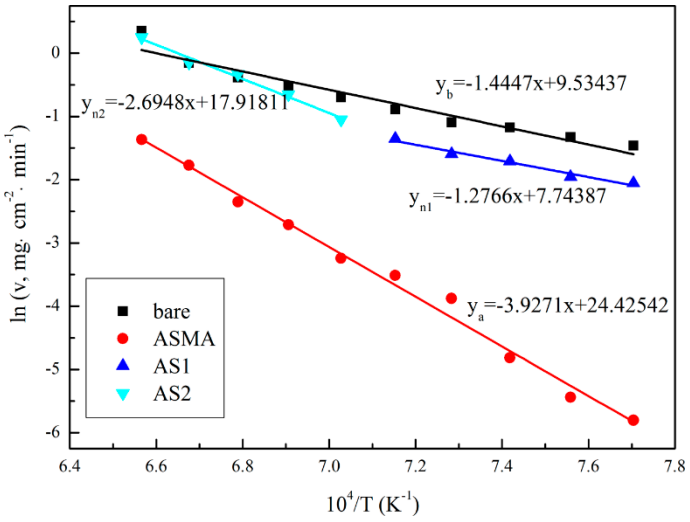

Figure 4. Results of non-isothermal kinetics.

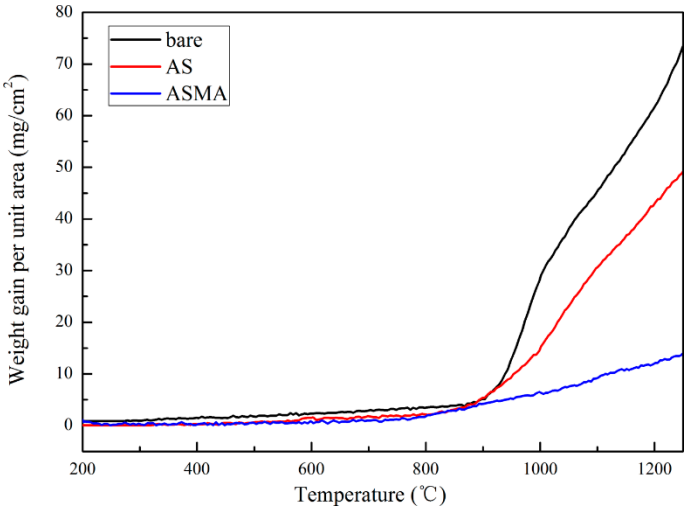

Figure 5. Results of continuous thermo-balance from 200 to 1250 °C with a rate of 10 °C/min.

Since the serious oxidation of carbon steel always occurred over 1250 °C, the isothermal kinetic was conducted at 1250 °C. It was widely accepted that the oxidation of carbon steel followed the parabolic law [3,23,24], which meant that the oxidation process was controlled by the diffusion. The reaction constant could be calculated by Equation (10) [2].

$$(\Delta\omega)^2 = \mathrm{H} + \mathrm{k_p} \times t_i \quad (10)$$

Here, t_i (s) is the duration of oxidation, $\Delta\omega$ is the weight gain per unit area (mg/cm^2), H is a constant, and k_p ($mg^2 \cdot cm^{-4} \cdot s^{-1}$) is the reaction rate constant.

In this study, the linear relationship between $\Delta\omega$ and $t_i^{1/2}$ was used to evaluate k_p [2]. As shown in Figure 6, the reaction rate constant (k_p) of the bare sample, the sample protected by AS, and the sample protected by ASMA was 2.09, 0.096, and 0.046 $mg^2 \cdot cm^{-4} \cdot s^{-1}$, respectively. It can be concluded that ASMA possessed a better anti-oxidation performance than AS due to its smaller reaction rate constant at 1250 °C.

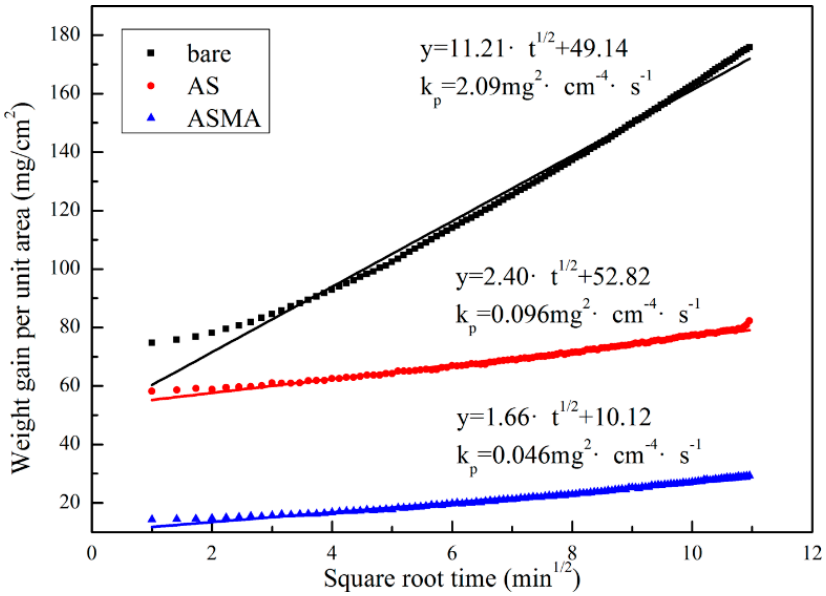

Figure 6. Results of isothermal kinetics.

3.2. Morphology of Coating

The microstructure was an intuitive evidence for evaluating the compactness of coating which controlled the inner diffusion rate of oxygen. Therefore, anti-oxidation performance of coating was better with a more compact structure. The outer-surface microstructures of sample protected by the ASMA and sample protected by the AS were investigated after the thermal treatments of different temperature (900, 1150, and 1250 °C). As described in Figure 7, ASMA formed a compact structure at 900 °C and the compactness improved with the increasing of temperature until 1250 °C. The amount of liquid phase increased with the rising temperature, the porosity reduced and thus the sintering of coating was enhanced at the same time. However, the sample protected by AS possessed a porous structure composed of isolated particles at 900 °C, while the compactness improved at 1150 °C. The above results suggested that SiO_2@Al could accelerate the sintering of the ceramic coating and enhance the compactness.

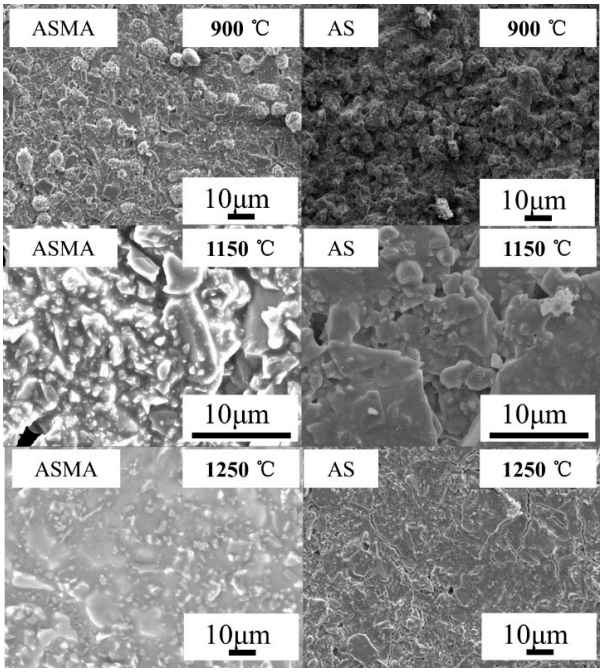

Figure 7. SEM images of outer-surfaces belonging to sample protected by ASMA and sample protected by AS at different temperatures.

3.3. Protection Mechanism

Figure 8 showed the TG-DTA data of the ASMA and AS slurry. As shown in Figure 8a, there was an endothermic peak at about 662.85 °C, an exothermic peak at 977.7 °C, and an exothermic peak at 1153.91 °C for ASMA slurry, while there was only a gradual exothermic trend during heating process for AS slurry. In order to interpret the possible reactions during the heating process, the phase transitions were investigated by XRD method at 500, 800, 1100, and 1250 °C, which were near the endothermic or exothermic temperature. Compared with Figure 9a,b, it was found that no specific phase formed between 500 and 800 °C, thus the endothermic peak at 662.82 °C could be attributed to the melting of Al powders in SiO_2@Al. Phases of Si and $Al_{3.21}Si_{0.47}$ were newly formed within ASMA when temperature increased from 800 to 1100 °C, which indicated that an exothermic reaction occurred as described in Equation (11) and it gave rise to the exothermic peak at 977.7 °C [25]. Compared with Figure 9c,d, it was remarkable that mullite and cristobalite formed within ASMA when temperature ranged from 1100 to 1250 °C. Therefore, the exothermic peak at 1153.91 °C might result from the exothermic reaction expressed as Equations (12) and (13) [26,27]. In contrast, there was no new phase formed within AS during the whole heating process except for cristobalite. To sum up, the Al powders in SiO_2@Al melted at 662.85 °C and reacted with SiO_2 on its surface, which generated local high temperature and the sintering of ceramic raw materials, thus contributing to its excellent anti-oxidation performance, which was consistent with the non-isothermal kinetics. Besides, mullite and cristobalite formed at 1150 °C could further enhance the coating compactness and improve the anti-oxidation performance above 1150 °C [19]. However, ceramic raw materials just sintered above 1150 °C within AS, and thus showed an unobvious anti-oxidation effect below this temperature.

$$4Al + 3SiO_2 \rightarrow 3Si + 2Al_2O_3 \quad (11)$$

$$SiO_2\ (\text{amorphous}) \rightarrow SiO_2\ (\text{cristobalite}) \quad (12)$$

$$3Al_2O_3 + 2SiO_2 \rightarrow 3Al_2O_3{\cdot}2SiO_2 \quad (13)$$

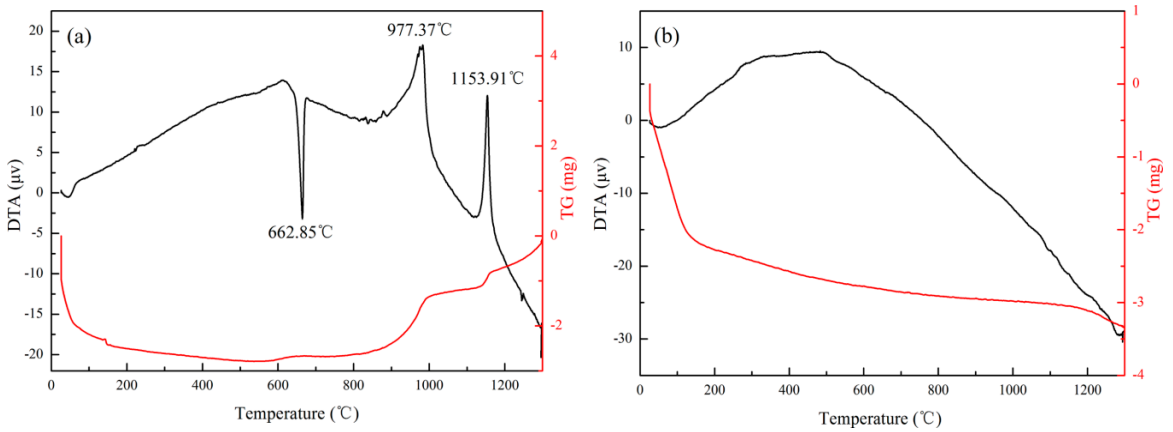

Figure 8. TG-DTA curves of (**a**) ASMA and (**b**) AS.

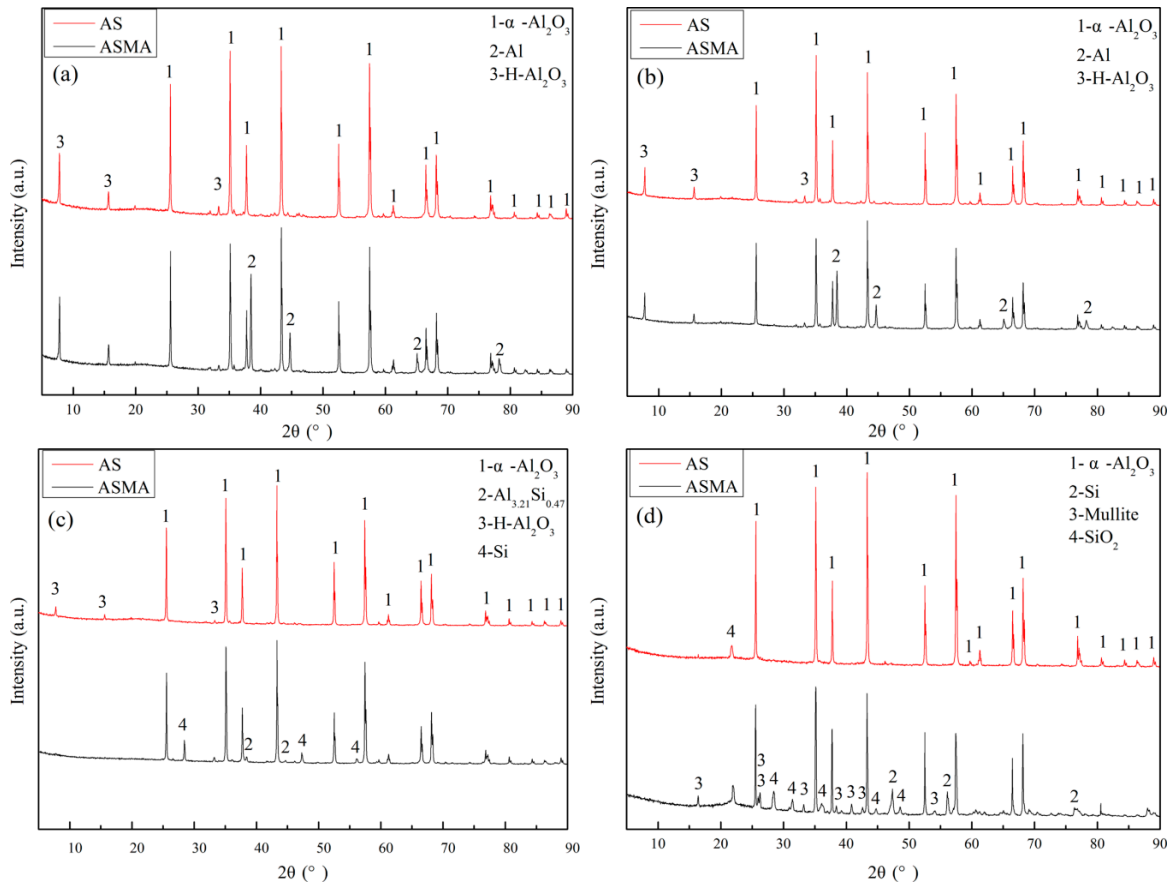

Figure 9. Comparisons of XRD result of the sample protected by ASMA and AS slurry at dffierent temperatures: (**a**) 500 °C, (**b**) 800 °C, (**c**) 1100 °C, (**d**) 1250 °C.

According to the SEM-EDS results of coating cross-sections exhibited in Figure 10, both the coatings were able to prevent the carbon steel substrate from oxidization at 1250 °C. Compared with Figure 11a,b, ASMA was composed of a hercynite layer, a mullite layer, and a ceramic layer with high aluminum content, while AS consisted of a Fe_3O_4 layer, an olivine layer composed of FeO and $2FeO{\cdot}SiO_2$, a ceramic layer composed of Al_2O_3 and cristobalite. Equations (14) or (15) possibly occurred to form the hercynite ($Al_2O_3{\cdot}FeO$) within ASMA. As reported in the literature [28], the structure of hercynite could be expressed as $(Fe^{2+}{}_{1-x}Al^{3+}{}_x)_{tet}(Al^{3+}{}_{2-x}Fe^{2+}{}_x)_{oct}O_4$ where $0 < x < 0.25$, while that of Fe_3O_4 could be expressed as $(Fe^{3+})_{tet}(Fe^{3+}Fe^{2+})_{oct}O_4$ [29]. Referring to Freer and O'Reilly [30], the diffusion activation energy of Fe^{2+} at octahedral site and tetrahedral site were 0.2($\pm$0.05) eV and 0.71

(±0.09) eV, which indicated that the diffusion of iron ions within hercynite was slower than Fe_3O_4 due to the lower fraction of Fe^{2+} occupied the octahedral site. Therefore, hercynite also played a significant role for enhancing the anti-oxidation ability of ASMA. However, hercynite was easily oxidized as shown in Equation (16) under oxidation condition. As mentioned in Section 3.1, the compactness of ASMA was greatly improved with the addition of SiO_2@Al, which effectively prohibited the inner diffusion of oxygen. As a result, the hercynite layer could be stable within the ceramic coating. The result agreed well with the finding in isothermal kinetic experiment.

$$3Al_2O_3 \cdot 2SiO_2 + 3FeO \rightarrow 3Al_2O_3 \cdot FeO + 6SiO_2 \quad (14)$$

$$Al_2O_3 + FeO \rightarrow Al_2O_3 \cdot FeO \quad (15)$$

$$4Al_2O_3 \cdot FeO + O_2 \rightarrow 4Al_2O_3 + 2Fe_2O_3 \quad (16)$$

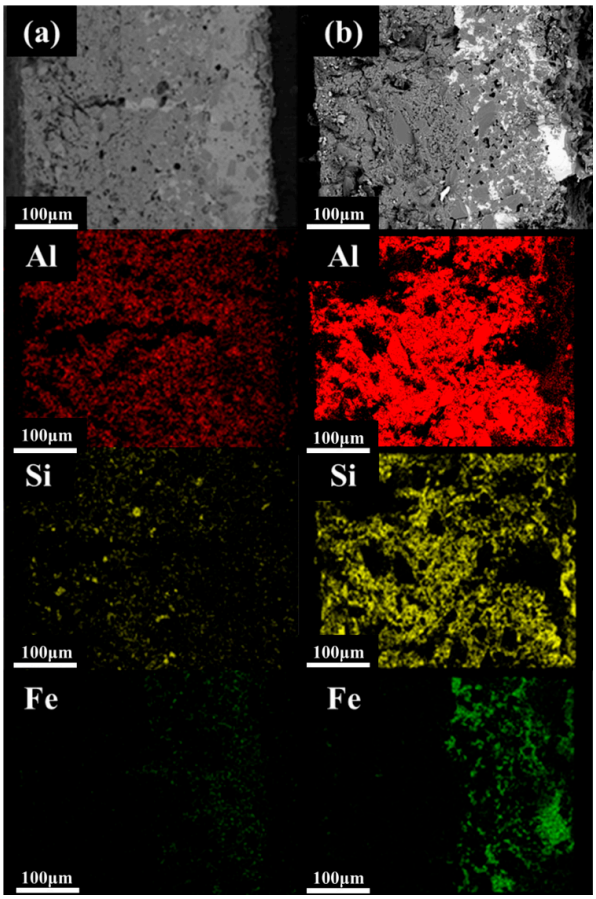

Figure 10. SEM-EDS images of cross-sections belonging to (**a**) the sample protected by ASMA and (**b**) the sample protected by AS at 1250 °C.

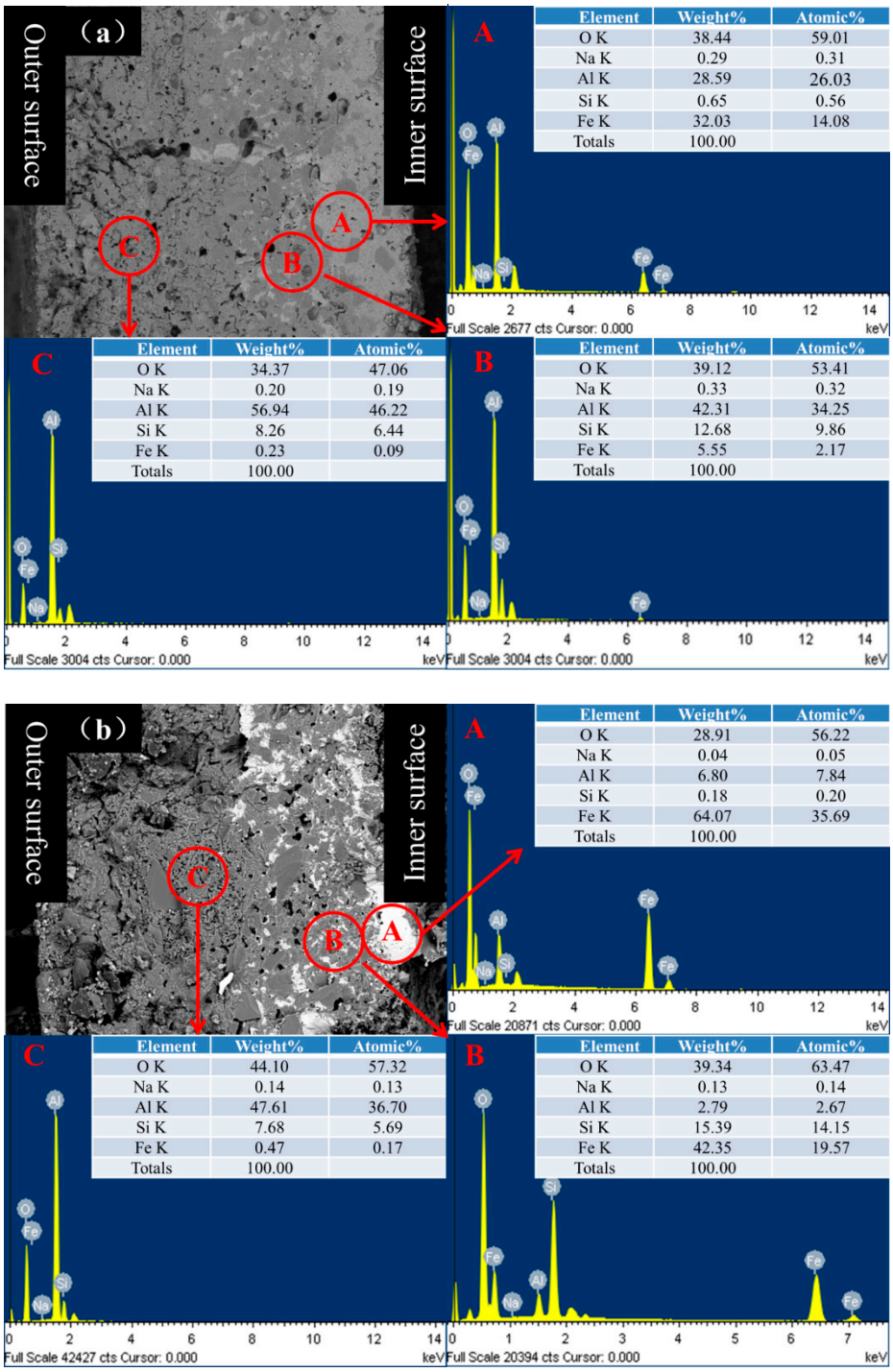

Figure 11. SEM images with results of EDS measurements performed on selected areas of cross-sections belonging to (**a**) sample protected by ASMA and (**b**) sample protected by AS at 1250 °C.

4. Conclusions

In present work, modified Al powders (SiO_2@Al) were prepared by the hydrolysis of tetraethyl orthosilicate (TEOS) under alkaline conditions. A new ceramic coating was prepared with the SiO_2@Al as additives to prevent the carbon steel from oxidization at 1250 °C. The anti-oxidation performance and a probable protective mechanism of the coating were clarified.

Some results were obtained as follows:

- The Al powders were successfully encapsulated by SiO_2 and the SiO_2@Al stably existed in the as-prepared alkaline coating slurry. The appropriate proportion of SiO_2@Al in the coating was 10%.
- The metallic Al in ASMA melted at 662.85 °C. What generated local high temperature and accelerated the sintering of ceramic raw materials was the exothermal reaction between the melted Al and SiO_2 ($4Al + 3SiO_2 \rightarrow 3Si + 2Al_2O_3$). The well-sintered structure decreased the inner diffusion rate of oxygen and enhanced the anti-oxidation effect of ASMA during the temperature-rise period.
- The hercynite layer formed within ASMA played a significant role for slowing down the external diffusion of iron ions due to the lower fraction of Fe^{2+} occupied the octahedral site, which facilitated the improvement of anti-oxidation ability at 1250 °C.

Author Contributions: Conceptualization, B.Y. and L.W.; Formal analysis, B.Y., G.Z. and L.W.; Funding acquisition, S.Y.; Investigation, B.Y., X.Z., Y.D. and L.W.; Methodology, B.Y., G.F. and L.W.; Software, G.Z.; Supervision, Y.C., Y.D. and S.Y.; Validation, B.Y. and Y.T.; Writing–original draft, B.Y.; Writing–review & editing, B.Y., Y.C. and L.W.

Funding: This research was funded by the National Strategic Priority Research Program 2017 (No. YFC0703205).

Conflicts of Interest: The authors declare no conflict of interest.

References

1. Frolenkov, K.Y.; Frolenkova, L.Y.; Shadrin, I.F. High-temperature oxidation of low-alloyed steel under glass coatings. *Prot. Met. Phys. Chem. Surf.* **2010**, *46*, 103–109. [CrossRef]
2. Fu, G.; Wei, L.; Zhang, X.; Cui, Y.; Wang, Y.; Yu, B.; Lv, C.; Ye, S. A MgO-SiO_2-Al_2O_3-ZnO ceramic-glass coating to improve the anti-oxidation of carbon steel at high temperature. *ISIJ Int.* **2018**, *58*, 929–935. [CrossRef]
3. Hu, X.J.; Zhang, B.M.; Chen, S.H.; Fang, F.; Jiang, J.Q. Oxide scale growth on high carbon steel at high temperatures. *J. Iron Steel Res. Int.* **2013**, *20*, 47–52. [CrossRef]
4. Liu, Y.; Zhang, W.; Tong, Q.; Sun, Q.; Chao, Y.; Yang, W.; Li, T.; Li, L. Effects of chemical composition on decarburization layer depth of high carbon steels in 2% oxygen atmosphere. *Heat Treat. Met.* **2017**, *42*, 143–148.
5. Heo, N.H.; Lee, J.K. Grain boundary segregation of phosphorus and intergranular surface cracking accompanied by decarburization in plain carbon steels. *ISIJ Int.* **2011**, *51*, 673–678. [CrossRef]
6. Torkar, M.; Glogovac, B. Diminution of scaling by the application of a protective coating. *J. Mater. Process. Technol.* **1996**, *58*, 217–222. [CrossRef]
7. Munther, P.; Lenard, J. The effect of scaling on interfacial friction in hot rolling of steels. *J. Mater. Process. Technol.* **1999**, *88*, 105–113. [CrossRef]
8. Mao, Z.L.; Yang, X.J.; Zhu, S.L.; Cui, Z.D.; Lu, Y. Pack cementation processing parameters for SiC coatings on C/C for optimum tribological properties. *Surf. Coat. Technol.* **2014**, *254*, 54–60. [CrossRef]
9. Fu, G.; Wei, L.; Shan, X.; Zhang, X.; Ding, J.; Lv, C.; Liu, Y.; Ye, S. Influence of a Cr_2O_3 glass coating on enhancing the oxidation resistance of 20MnSiNb structural steel. *Surf. Coat. Technol.* **2016**, *294*, 8–14. [CrossRef]
10. Fu, G.Y.; Wei, L.Q.; Zhang, X.M.; Cui, Y.B.; Lv, C.C.; Ding, J.; Yu, B.; Ye, S.F. A high-silicon anti-oxidation coating for carbon steel at high temperature. *Surf. Coat. Technol.* **2017**, *310*, 166–172. [CrossRef]
11. Wei, L.; Peng, L.; Ye, S.; Xie, Y.; Chen, Y. Preparation and properties of anti-oxidation inorganic nano-coating for low carbon steel at an elevated temperature. *J. Wuhan Univ. Technol.* **2006**, *21*, 48–52.
12. Wang, D. Formation and property of ceramic layer on a low-carbon steel. *Int. J. Process. Sci. Charact. Appl. Adv. Mater.* **2007**, 134–138.
13. Zhou, X.; Ye, S.F.; Xu, H.W.; Liu, P.; Wang, X.J.; Wei, L.Q. Influence of ceramic coating of MgO on oxidation behavior and descaling ability of low alloy steel. *Surf. Coat. Technol.* **2012**, *206*, 3619–3625. [CrossRef]
14. Zhou, X.; Wei, L.Q.; Liu, P.; Wang, X.J.; Ye, S.F.; Chen, Y.F. Preparation and characterization of high temperature protective ceramic coating for plain carbon steel. *Chin. J. Process Eng.* **2010**, *10*, 167–172.

15. Li, G.; Jie, X.; He, L. High temperature oxidation behavior of (Ti,Al) C ceramic coatings on carbon steel prepared by electrical discharge coating in kerosene. *Adv. Mat. Res.* **2011**, *189–193*, 186–192. [CrossRef]
16. Nguyen, M.D.; Bang, J.W.; Kim, Y.H.; Bin, A.S.; Hwang, K.H.; Pham, V.H.; Kwon, W.T. Slurry spray coating of carbon steel for use in oxidizing and humid environments. *Ceram. Int.* **2018**, *44*, 8306–8313.[CrossRef]
17. Wang, C.; Chen, S. The high-temperature oxidation behavior of hot-dipping Al–Si coating on low carbon steel. *Surf. Coat. Technol.* **2006**, *200*, 6601–6605. [CrossRef]
18. Yang, C.H.; Lin, S.N.; Chen, C.H.; Tsai, W.T. Effects of temperature and straining on the oxidation behavior of electrical steels. *Oxid. Met.* **2009**, *72*, 145–157. [CrossRef]
19. Ren, Q.; He, X.; Wu, X. Effects of nano-additives on the structure and properties of 99% alumina ceramics. *Rare Met. Mater. Eng.* **2008**, *37*, 452–454.
20. Yin, J.; Wang, X.; Zhang, Y.; Zhao, C.; Wang, X.; Gao, H.; Yang, J. Effect of sintering aids on high purity alumina ceramic densification process. *Chin. Rare Earths* **2014**, *35*, 16–20.
21. Chen, R.Y.; Yuen, W.Y.D. The effects of steel composition on the oxidation kinetics, scale structure, and scale-steel interface adherence of low and ultra-low carbon steels. *Mater. Sci. Forum* **2006**, *522–523*, 451–460. [CrossRef]
22. Le, M.T.; Kim, C.; Lee, J. Effect of silica addition on ceramic layer in centrifugal-thermit reaction. *Mater. Trans.* **2008**, *49*, 1410–1414. [CrossRef]
23. Jiang, Z. Research on TG-DSC of carbon steel oxidation kinetics. *Hot Work. Technol.* **2015**, *44*, 89–91.
24. Nagelberg, A.S. Observations on the role of Mg and Si in the directed oxidation of Al-Mg-Si alloys. *J. Mater. Res.* **1992**, *7*, 265–268. [CrossRef]
25. Aksay, I.A.; Pask, J. A stable and metastable equilibria in system SiO_2-Al_2O_3. *J. Am. Ceram. Soc.* **1975**, *58*, 507–512. [CrossRef]
26. Zhu, Z.; Wei, Z.; Sun, W.; Hou, J.; He, B.; Dong, Y. Cost-effective utilization of mineral-based raw materials for preparation of porous mullite ceramic membranes via in-situ reaction method. *Appl. Clay Sci.* **2016**, *120*, 135–141. [CrossRef]
27. Odashima, H.; Kitayama, M. Oxidation-inhibition mechanism and performance of a new protective coating for slab reheating of 3% Si-steel. *ISIJ Int.* **1990**, *30*, 255–264. [CrossRef]
28. Dong, Y.; Lu, H.; Cui, J.; Yan, D.; Yin, F.; Li, D. Mechanical characteristics of $FeAl_2O_4$ and $AlFe_2O_4$ spinel phases in coatings—A study combining experimental evaluation and first-principles calculations. *Ceram. Int.* **2017**, *43*, 16094–16100. [CrossRef]
29. Hazen, R.M.; Jeanloz, R. Wüstite ($Fe_{1-x}O$): A review of its defect structure and physical-properties. *Rev. Geophys.* **1984**, *22*, 37–46. [CrossRef]
30. Freer, R.; Oreilly, W. The diffusion of Fe^{2+} ions in spinels with relevance to the process of maghemitization. *Miner. Mag.* **1980**, *43*, 889–899. [CrossRef]